Bulletin of the Seismological Society of America, Vol. 105, No. 2A, pp. 568–579, April 2015, doi: 10.1785/0120140147

The Earthworm Based Earthquake Alarm Reporting System in Taiwan

by Da-Yi Chen,* Nai-Chi Hsiao, and Yih-Min Wu

Abstract For more than 10 years, the Central Weather Bureau of Taiwan has operated an earthquake early warning (EEW) system and has issued warnings for specific agencies. For the past two years, the Earthworm platform has been used to integrate real-time seismic data streams from different types of seismic stations and to monitor seismicity in Taiwan. Using the Earthworm platform, the Earthworm Based Earthquake Alarm Reporting (*e*BEAR) system is currently in development for shortening reporting times and improving the accuracy of warnings for EEW purposes. The *e*BEAR system consists of new Earthworm modules for managing *P*-wave phase picking, trigger associations, hypocenter locations, magnitude estimations, and alert filtering prior to broadcasting. Here, we outline the methodology and performance of the *e*BEAR system. To calibrate the *e*BEAR system, an offline test was implemented using 154 earthquakes with magnitudes ranging from M_L 4.0 to 6.5. In a comparison of online performance using the current EEW system, the *e*BEAR system reduced reporting times and improved the accuracy of offshore earthquake locations and magnitudes. Online performance of the *e*BEAR system indicated that the average reporting times afforded by the system are approximately 15 and 26 s for inland and offshore earthquakes, respectively. The *e*BEAR system now delivers warnings to elementary and junior high schools in Taiwan.

Introduction

An earthquake early warning (EEW) system is a practical tool for mitigating earthquake hazards. EEW systems are capable of estimating the occurrence time, location, and magnitude of an earthquake and of issuing warnings before strong ground shaking hits a target area. With timely information, people and manufacturing facilities are able to take the necessary precautions to reduce the seismic hazards caused by large earthquakes. EEW systems have been tested or are currently in use in many countries with high earthquake hazards (Allen *et al.*, 2009).

Taiwan is located on one of the most active seismic zones in the world, in an area where the Philippine Sea plate moves toward the Eurasia plate at approximately 7 cm/yr (Yu *et al.*, 1997). When two tectonic plates collide, stresses accumulate then cause earthquakes. The largest damaging inland earthquake to strike Taiwan in the past 20 years was the 1999 M_w 7.6 Chi-Chi earthquake (Shin and Teng, 2001). Because of rapid urbanization in Taiwan, seismic risks have recently increased. For example, the 2002 M_w 7.1 eastern Taiwan offshore earthquake caused strong ground shaking inside the Taipei basin (Huang *et al.*, 2010). During strong ground shaking, a crane operating on top of the construction area of the Taipei 101, the tallest building in Taiwan (508 m tall), crashed and dropped to the ground. The 2010 M_w 6.3 Jiasian earthquake brought strong ground motions to southern Taiwan, causing an operating Taiwan High Speed Rail train to run off its tracks (Huang *et al.*, 2011; Wu *et al.*, 2011). Given these types of incidents in Taiwan, a reliable and fast EEW system is urgently needed to provide early warnings for the next large earthquake.

Over the years, many studies have been conducted regarding the development of an EEW system in Taiwan. In 1995, an earthquake rapid reporting system began operating on the basis of 16-bit strong-motion seismometers and was a type of early-stage EEW system for Taiwan (Wu *et al.*, 1997). Although the system could not issue warnings prior to large ground shaking, it provided rapid reporting within 102 s for the Chi-Chi earthquake and was the leading technology at that time (Wu *et al.*, 2000). As EEW system necessity demanded, the Central Weather Bureau (CWB) was the first to test an EEW prototype system within the Hualien area in Taiwan. To reduce reporting times and provide early warnings for distant metropolitan regions, a new idea, based on the prototype system, was proposed for applying the subnetwork method to earthquake monitoring (Wu *et al.*, 1999). Using the subnetwork concept and M_{L10}, a quick magnitude determination method (Wu *et al.*, 1998) that adopted 10 s records following the first *P*-wave arrival, the current EEW system (the virtual subnetwork [VSN] system) was built and

*Also at Department of Geosciences, National Taiwan University, No. 1, Section 4, Roosevelt Road, Taipei 10617, Taiwan.

achieved an average 22 s reporting time (the time between an earthquake's origin time and the time the EEW system issues a report) (Wu and Teng, 2002). However, due to the limits of the M_{L10} method, the reporting time could not be reduced to within 10 s. To further reduce reporting times, the *P*-wave method, based on the peak amplitude of displacement records (P_d) for the vertical component using a 3 s time window for magnitude determinations (Wu and Zhao, 2006), was tested and operated (Hsiao *et al.*, 2009, 2011). The CWB has recently upgraded seismic facilities within the original seismic network and deployed 30 borehole stations, as well as one cable-based ocean-bottom seismic station. At the same time, to enhance the density and coverage of station distributions, real-time seismic data streams from various seismic networks were integrated using the Earthworm platform, a program originally developed by the U.S. Geological Survey (Johnson *et al.*, 1995). Based on the above, an Earthworm-based EEW prototype system was constructed and has been tested since 2007 (Hsiao *et al.*, 2011; Chen *et al.*, 2012).

To enhance data-processing capabilities and reduce reporting times, we propose the use of the Earthworm Based Earthquake Alarm Reporting (*e*BEAR) system within the current EEW system. The algorithms of the *e*BEAR system, which provide earthquake parameters and filtering alerts, were developed by performing an offline test using 154 events with magnitudes ranging from 4.0 to 6.5. To determine whether or not the *e*BEAR system was capable of a higher level of performance, we also compared the online performance of the VSN and *e*BEAR systems. The *e*BEAR system is currently operated by the CWB and since January 2014 has broadcasted warnings to elementary and junior high schools in Taiwan.

The Seismic Network in Taiwan

Currently, two seismic networks are operated within the CWB. The first network, the Real-Time Data stream (RTD) seismic network, consists of 110 stations equipped with one Geotech Smart24A seismometer that transmits real-time, strong-motion data to the CWB via 4800-baud leased telephone lines. Each telemetered signal is digitized at 50 samples per second using a 16-bit resolution. The current EEW system, VSN, operates within this seismic network. The second, the Central Weather Bureau Seismic Network (CWBSN), is an upgraded and integrated network that improves data quality, station coverage, and density by integrating various types of seismic stations and seismic networks from other institutes. The *e*BEAR system is operated under the CWBSN. The station distribution of the CWBSN, which integrates different types of seismic stations operated by the CWB and the Institute of Earth Sciences (IES) of Academia Sinica (which provides waveforms for 23 stations from the Broadband Array in Taiwan for Seismology), is shown in Figure 1. In addition, using a connection to buffer uniform data of the Incorporated Research Institutions of Seismology (IRIS), one Japanese station (YOJ) has been merged into the monitoring network and has improved station coverage within the eastern offshore region of Taiwan. Each real-time seismic signal, digitized at 24-bit resolution and obtained using time stamps from a Global Positioning System, is packed and transmitted to CWB headquarters in Taipei via Ethernet or Internet. With the exception of IRIS data at 20 samples per second, digital signals are digitized at 100 samples per second.

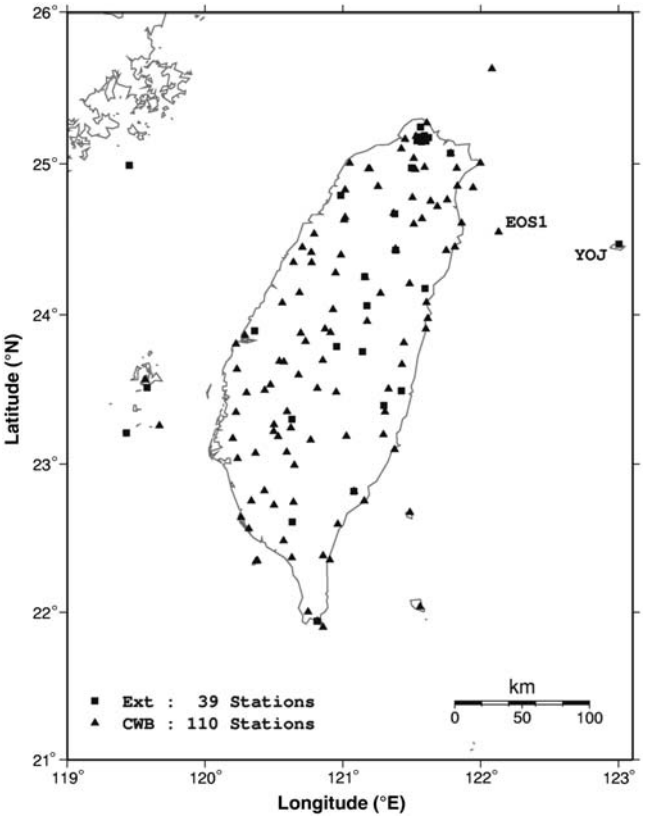

Figure 1. The station distribution of the Central Weather Bureau (CWB) Seismic Network. EOS1 is the cable-based ocean-bottom seismic station. YOJ is the Japanese station. Ext indicates stations operated by external institutions.

The CWBSN consists of four types of seismic stations including six-channel seismic stations, broadband seismic stations, borehole seismic stations, and one cable-based ocean-bottom seismic station. Among seismic stations, some have been upgraded from older types, while others have been newly added. Six-channel seismic stations were upgraded and combined from original short-period and strong-motion instruments, digitized at 12- and 16-bit resolutions, respectively (Teng *et al.*, 1997). Prior to station upgrades, two types of instruments were operated separately and transmitted data through telephone lines; signal time was stamped by the central station (Chang *et al.*, 2012). Since 2007, using Geotech Smart24A accelerometers to replace the original instruments (Geotech A900A) and to connect Teledyne Geotech S13 short-period sensors, the CWB has combined these two types of seismic signals. As a result, 70 upgraded six-component

stations have been constructed, each hosting three-component short-period velocity sensors and one three-component strong-motion sensor.

For EEW purposes, the data loggers located at broadband seismic stations were replaced using modern equipment capable of sending seismic waveforms with a 1 s packet length. The system consists of 23 stations that use one three-component broadband seismograph. To prevent clipped waveforms caused by near-field strong shakings, most stations are equipped with an additional three-component strong-motion sensor. Such high-quality waveforms are also used to obtain centroid moment tensor (CMT) solutions (Shin *et al.*, 2013).

In addition, 30 borehole seismic stations are operational. Each hosts a three-component strong-motion seismograph on the surface and a three-component strong-motion seismograph, as well as a broadband seismograph within boreholes at a depth of approximately 300 m from the surface. Seismic signals from borehole seismometers provide waveforms with a high signal-to-noise ratio, useful for improving the accuracy of phase picking. Since 2008, the number of borehole seismic stations has increased by approximately five stations each year. In the near future, the total number of borehole stations will increase to 70.

In November 2011, the first cable-based ocean-bottom seismometer, the Marine Cable Hosted Observatory (MACHO), began operating in Taiwan. The MACHO has one seismic station located within the northeastern offshore area of Taiwan, with a cable line length of 45 km, and hosts a three-component strong-motion accelerometer and a three-component broadband seismograph (Hsiao *et al.*, 2013). The MACHO is very expensive, and only one station is currently in operation. However, because the Philippine Sea plate subducts beneath the Eurasia plate of northeastern Taiwan and since many large earthquakes have occurred in this area in the past, the MACHO system is critical to the EEW system. The MACHO is capable of detecting seismic waves faster than inland stations.

Figure 2 provides the system configuration of the CWBSN for a three-layer structure within the data-processing center used for the acquisition, integration, and application of real-time seismic signals. In the first layer, real-time seismic data streams are packaged and transmitted from field stations or external seismic networks then received by commercial software or Earthworm via various Internet Protocol (IP)-based networks. SMARTGeoHub and Scream software packages are used to receive real-time seismic waveforms from instruments made by Geotech and Güralp, respectively. Seismic waveforms from external seismic networks provided by IES and IRIS are received using the Earthworm modules IMPORT_ACK and SLINK2EW, respectively.

In the second layer, an Earthworm cluster integrates seismic data streams from different seismic instruments and provides two types of seismic waveforms. One waveform type, WAVE_SERVERV, can store and provide seismic waveforms over a period of time and is used for data displays and archives. The second waveform type, EXPORT_ACK,

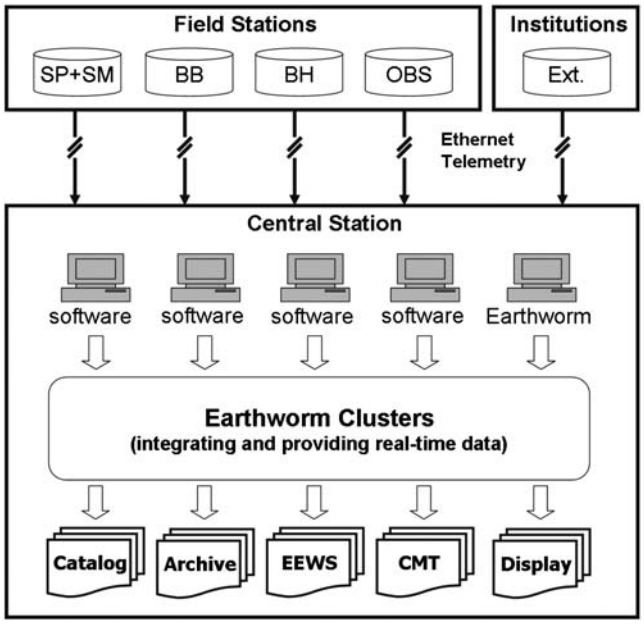

Figure 2. A schematic diagram of the data-processing center. SP, short-period stations; SM, strong-motion stations; BB, broadband stations; BH, borehole stations; and OBS, cable-based ocean-bottom seismic stations. Ext indicates stations operated by external institutions.

can provide data streams much faster than the previous one and is used for real-time data processing. For system backup, two computers running WAVE_SERVERV and three computers running EXPORT_ACK are operated in parallel.

In the third layer, also called the application layer, several tasks are performed. These include EEW operation, the generation of products obtained from the earthquake catalog and the CMT, the maintenance of the seismic waveform data archive, and the display.

Via its modules and shared memory regions, the Earthworm system is designed for automatic seismic data processing (Johnson *et al.*, 1995). Each module has specific tasks such as data acquisition, processing, and archiving. Adopting shared memory regions makes it convenient for each module to easily receive or broadcast messages such as waveform data, *P*-wave arrivals, hypocenter, and magnitude. Earthworm prepares seismic-related modules and is open source. Therefore, users can use existing modules or create new modules for specific purposes.

Configuration of the *e*BEAR System

An Earthworm diagram that describes data flow within the *e*BEAR system is provided in Figure 3a. For system calibration, we ran the system in offline mode using the TANKPLAYER module. To receive real-time data for online operations, we applied the IMPORT module. The three circles provided in Figure 3a represent shared memories within Earthworm. The first shared memory, WAVE_RING, contains waveform data that can be processed using the

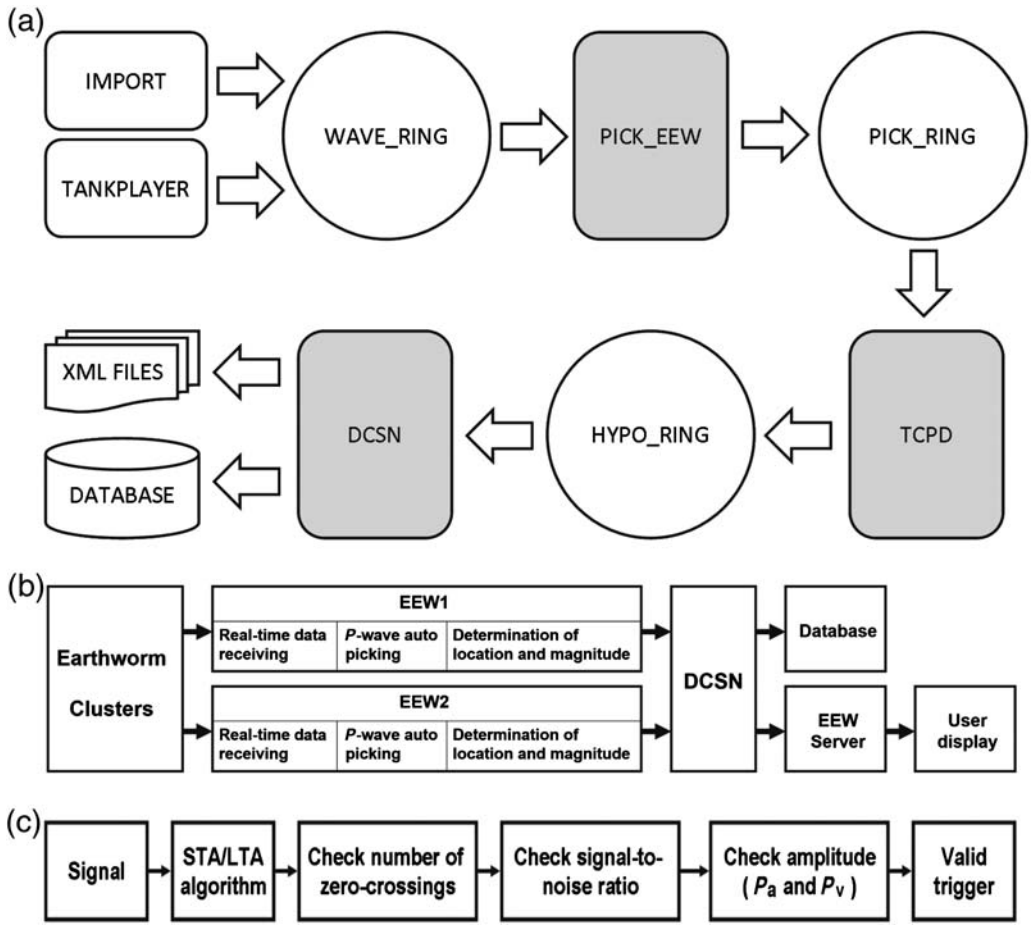

Figure 3. The configuration of the Earthworm Based Earthquake Alarm Reporting (*e*BEAR) system. (a) A flowchart for data processing within the *e*BEAR system. (b) The hardware configuration of the *e*BEAR system. (c) A flowchart of the algorithms designed for the PICK_EEW module. The rectangles represent different computers.

PICK_EEW module to determine *P*-wave arrivals, as well as the peak amplitudes for *P*-wave displacement (P_d), velocity (P_v), and acceleration (P_a) within a 3 s time window. The second shared memory, PICK_RING, not only contains information from the PICK_EEW module, but also provides information to the TCPD module for generating earthquake messages, including source parameters. When an earthquake occurs, the TCPD module may update information for the event and create earthquake messages. Updated earthquake messages are stored within the third shared memory, HYPO_RING. At the end of the process, the DCSN module filters earthquake messages using specific criteria (as discussed later) and generates EEW reports for broadcasting as an XML-formatted file.

Figure 3b provides the hardware configuration of the *e*BEAR system. For system backup, we designed two parallel EEW units, EEW1 and EEW2 that run the same procedure and data for generating earthquake messages. When an earthquake occurs, both EEW1 and EEW2 send earthquake messages to the system running the DCSN module. Only the first system sending the earthquake message is activated within the DCSN module. After receiving an earthquake message, the DCSN module writes an XML-formatted file onto the EEW server used to broadcast EEW reports to end users; then, to warn the end user, a display program pops up on the computer screen.

P-Wave Arrival Picking

The original Earthworm module, PICK_EW, requires time to check the seismic coda term within the autopicking procedure. The work is time consuming and not suitable for EEW systems. Therefore, we created a new module named PICK_EEW by revising the module and autopicking the procedure to run without checking the seismic coda term. To avoid false pickings caused by background noise, we also added two parameters, P_a and P_v. Because seismic waveforms from field stations have different noise levels depending on vibrations from the natural environment or artificial activities, these two parameters can be used as thresholds for ignoring spikes caused by noise. Table 1 provides the parameters we used in the PICK_EEW module of the *e*BEAR system.

Figure 3c displays the procedure for *P*-wave autopicking. The PICK_EEW module declares possible picks based

Table 1
The Parameters for *P*-Wave Phase Picking *e*BEARS Picker (PICK_EEW)

Parameters	Short Description	Default Value
MinSmallZC	Defines the minimum number of zero crossings for a valid pick within the first second after *P*-wave arrival	3 for broadband or 5 for acceleration
MaxMint	The maximum interval (in samples) between zero crossings	100
RawDataFilt	Sets the filter parameter RawDataFilt applied to the raw trace data	0.939
CharFuncFilt	Sets the filter parameter CharFuncFilt applied during calculations of the characteristic function of waveform data	3
StaFilt	Sets the filter parameter (time constant) StaFilt used in the calculation of the short-term average (STA) of the characteristic function of the trace	0.6
LtaFilt	Sets the filter parameter (time constant) LtaFilt used in the calculation of the long-term average (LTA) of the characteristic function of the trace	0.15
EventThresh	Sets the STA/LTA event threshold	5
RmavFilt	The filter parameter (time constant) used to calculate the running mean of the absolute value of the waveform data	0.9961
DeadSta	Sets the dead station threshold (counts)	1,000,000
MinPa	Defines the minimum value of peak amplitude for acceleration for a valid pick	0.01
MinPv	Defines the minimum value of peak amplitude for velocity for a valid pick	0.0001

on the short-term average (STA) and long-term average (LTA) algorithm. To become a candidate pick of a seismic trace, the ratio of STA/LTA should be greater than two times a certain threshold. Following a pick based on the threshold, and to distinguish ground noise and the seismic signal, we considered three additional conditions: the number of zero crossings, the signal-to-noise ratio, and the P_a and P_v. Using this procedure, the module was able to qualify the candidate pick as a valid seismic pick. In practice, because each seismic station has different background noise, we tested different sets of picking parameters by performing an offline test.

Hypocenter and Magnitude Determinations

After the TCPD modules jointly trigger using a space–time window based on expected travel times, the event hypocenter is estimated using two steps. For determining the event epicenter, the module first adopts Geiger's method, an inversion process using a half-space velocity model in which velocity linearly increases with depth. For estimating event depth, the module then uses a grid search method with depths ranging from 10 to 100 km in steps of 10 km. Theoretical travel times to each station are calculated and compared to those observed at each depth. Finally, the depth with minimum residuals and the epicenter determined by Geiger's method are considered as the event hypocenter.

The procedure is performed within the TCPD module via an updating process. At the beginning of the process, after at least six picks of seismic waveforms, the TCPD module begins to locate an event. When the root mean square (rms) of travel-time residuals resulting from the inversion process is larger than 0.8, the pick with the largest travel-time residuals is removed and the inversion process is again performed. When additional picks of seismic waveforms participate, the procedure of hypocenter determination is repeated and the estimated hypocenter is updated.

Earthquake magnitudes are predicted using the initial portion of *P*-wave peak displacement P_d within the 3 s time window. Following a double-integrated, strong-motion, and integrated broadband, the PICK_EEW module applies a 0.075 Hz high-pass filter to displacement records. The P_d value is then used to estimate magnitude (M_{P_d}) based on the empirical formula of Hsiao *et al.* (2011). The empirical formula for borehole stations has not yet been established. In addition, since the frequency response of the short-period sensor is approximately 1 Hz, short-period signals may underestimate the P_d value for large earthquakes. Only broadband and strong-motion sensors on the surface are used for P_d determinations within the EEW system.

Earthquake magnitude is estimated by obtaining an average for each M_{P_d} value from each seismic station. However, the false picking of *P*-wave arrivals, the directivity effect, and site effects may lead to unreasonable M_{P_d} values. For obtaining robust estimations of magnitude and to reduce errors, three steps are applied. First, only M_{P_d} values within one standard deviation of the dataset are used. Next, each record is weighted according to *P*-wave travel-time residuals. The weighting factor is expressed as

$$W_i = \left(\frac{1}{1 + |R_i|}\right)^2, \tag{1}$$

in which W_i is the weighting factor of each M_{P_d} value and R_i (in seconds) is the *P*-wave travel-time residual for each corresponding M_{P_d} value. Finally, a weighted average for obtaining earthquake magnitude is expressed as

$$M = \sum\left(\frac{W_i}{\sum W_i} \times X_i\right), \tag{2}$$

in which X_i is the M_{P_d} value for each station.

Figure 4. Graphical output of the *e*BEAR system during a simulation of the M_L 6.5 earthquake in central Taiwan. (top left) The origin event time and the name of the target city. (center) The square represents the target area, the black line represents the wavefront of the *P* wave, and the white line represents the wavefront of the *S* wave. (center right) The countdown timer for the *S*-wave arrival. (top right) The predicted intensity in the target area. The color version of this figure is available only in the electronic edition.

EEW Reports

When an earthquake occurs, the number of seismic picks are increased as seismic waves propagate away from the epicenter. As a result, the TCPD module determines the earthquake message and continuously updates that message. We propose that the numbers of updating earthquake messages will increase quickly and will be significant for large and local earthquakes. In contrast, for small earthquakes or for noise, the number of updating earthquake messages will increase slowly and will be small. Therefore, if the EEW system determines a large number of updating earthquake messages for an ongoing earthquake, we consider the EEW information as a reliable warning.

To prevent false alarms, the DCSN module always skips the first and second earthquake message generated from the TCPD module. The third earthquake message is the first EEW report to users. The EEW report is written in an XML-formatted file for broadcasting. The EEW report is updated either when differences in the magnitude or the epicenter are larger than 0.5 or 20 km, respectively, as compared to the last EEW report.

Figure 4 provides a user display that pops up automatically when an XML-formatted message is received. The display estimates the seismic intensity, the wavefronts of *P*- and *S* waves, and the remaining warning time (defined as the time between the reporting time and the arrival of the *S* wave to the target area). If the EEW report is updated, the user display directly changes the location of the epicenter and again re-estimates EEW-related parameters.

The Offline Test and Online Performance Comparison

To calibrate the *e*BEAR system, an offline test was implemented in this study. From 2012 to 2013, we collected recorded seismic waveforms with magnitudes greater than 4.0, depths less than 40 km, and epicenters within 40 km of the coastline of Taiwan based on the upgraded CWBSN. A total of 154 seismic events, including four events with magnitudes between 6.0 and 6.5, were used in the test. The results, including earthquake locations and magnitudes, were compared to the CWB earthquake catalog. The reporting time of the offline test (defined as the time the EEW report is issued following the event origin time) does not include a telemetry delay of within 2 s. Figure 5 provides the offline performance of the *e*BEAR system in comparison with the results from the CWB catalog. The average errors for epicenter and focal depth locations are 4.2 and 5.3 km, respectively. The standard deviation of the local magnitude is 0.3 units. The average reporting time is 14.7 s. Some events located in southwestern Taiwan with relatively higher station density

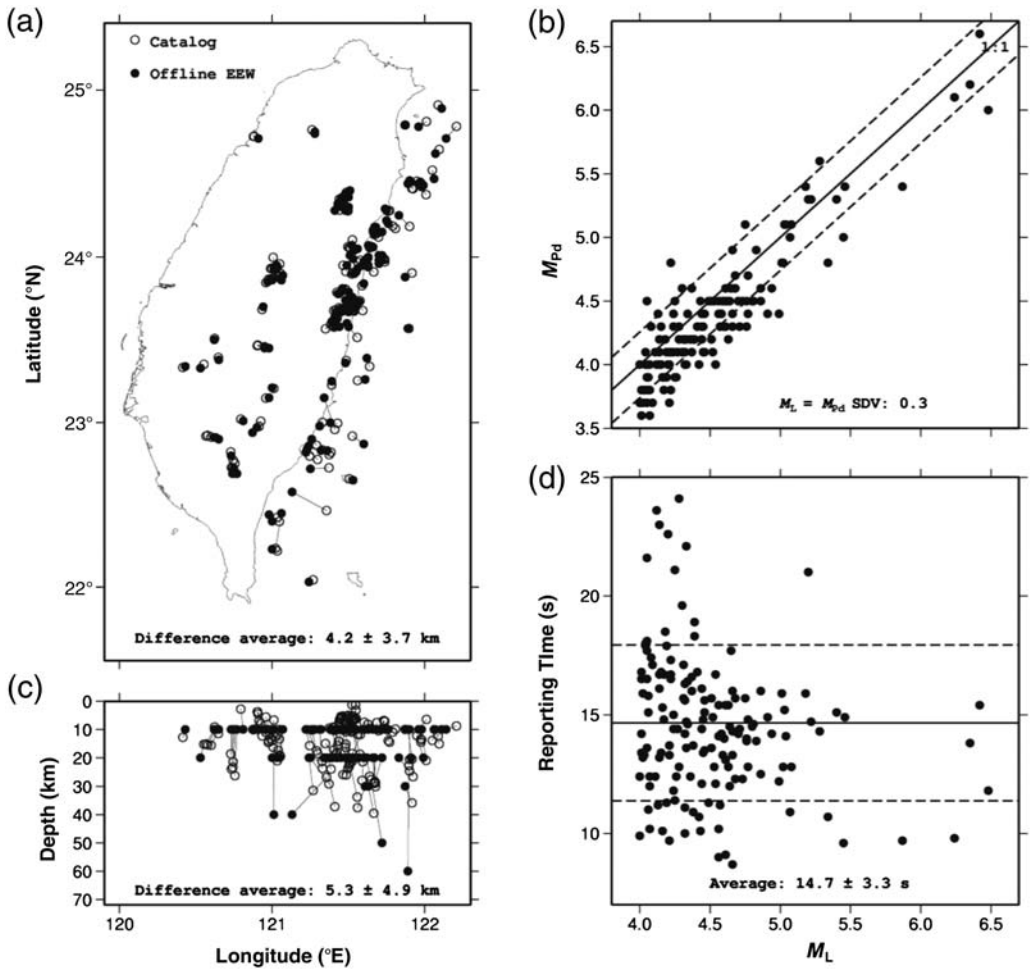

Figure 5. A comparison between the offline test and the CWB published catalog, as follows: (a) the epicenters, (b) the magnitudes, (c) the focal depths, and (d) the reporting time of the offline test. Open circles represent earthquake locations obtained from the published CWB catalog, and solid circles represent earthquake locations from the *e*BEAR system.

and coverage may be reported within 10 s. The offline results are acceptable for EEW purposes and suggest three points. First, the two-step method for determination of the epicenter and focal depth is suitable for a complicated tectonic environment such as Taiwan. Second, using a P_d value within a 3 s time window following *P*-wave arrival is useful for measuring the size of moderate-sized earthquakes with magnitudes ranging from 4.0 to 6.5. Third, when an earthquake occurs in an area with a relatively higher station density and coverage, the number of updating earthquake messages quickly increases within the *e*BEAR system. For this type of event, the system is able to obtain a third earthquake message (an EEW report) within a short period of time. For further discussion of the reporting time, Figure 6 provides the relationship between the reporting time and the station coverage gap. For most inland events with a station coverage gap generally less than 150°, reporting can occur within 15 s. On the other hand, for offshore events the reporting times may take more than 20 s when the station coverage gap is greater than 200°. The results indicate that currently the station cov-

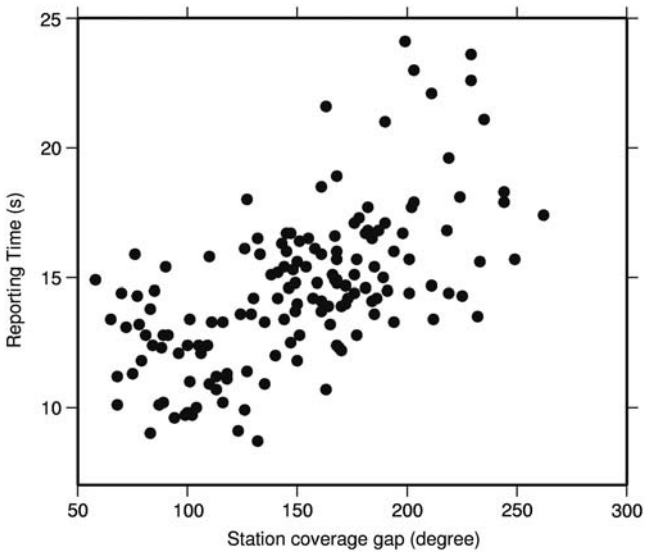

Figure 6. The relationship between reporting time and station coverage gap.

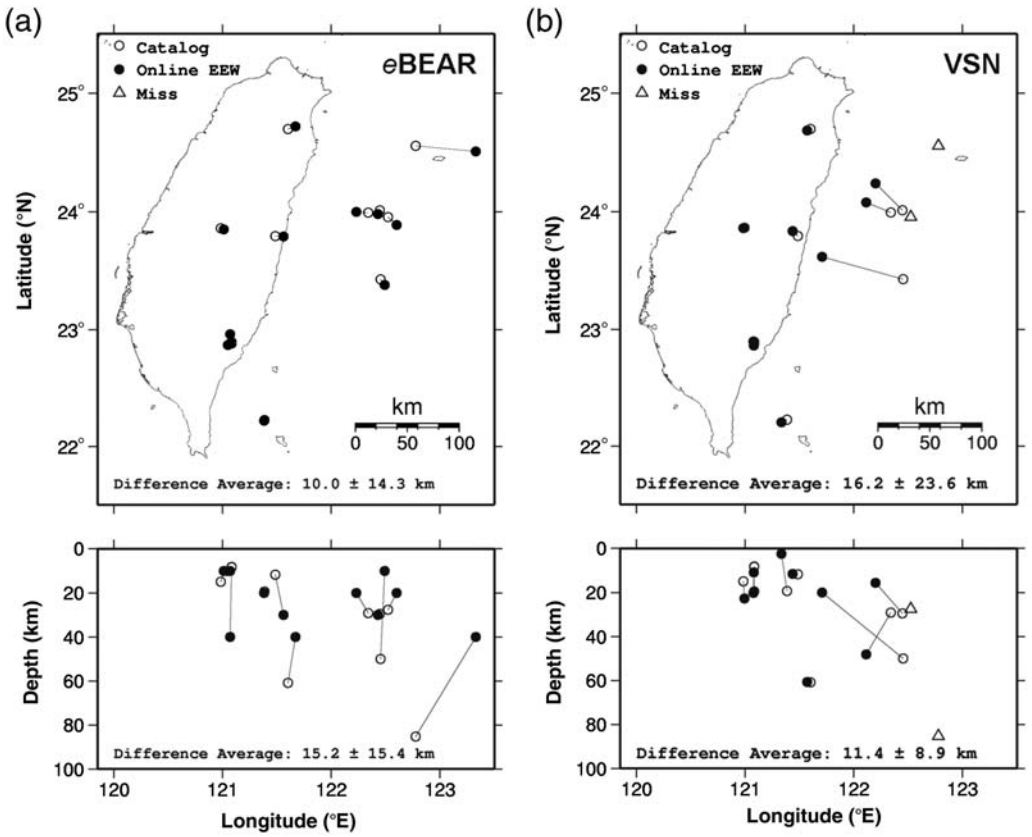

Figure 7. Location estimations as compared to online performance between the *e*BEAR and virtual subnetwork (VSN) systems: (a) the epicenter distribution of the CWB catalog and events of the earthquake early warning (EEW) alarms and missed alarms from the *e*BEAR system, and (b) the epicenter distribution of the CWB catalog and events of the EEW alarms and missed alarms from the VSN system. Open circles represent earthquake locations from the published CWB catalog, solid circles represent earthquake locations from the EEW system, and open triangles represent missing reports from the EEW system.

erage gap is a key factor for controlling the reporting time of the *e*BEAR system.

For an online system comparison between the VSN and *e*BEAR systems, we collected online operating performance data from January to March of 2014. Figure 7a,b indicates that the *e*BEAR system had no missed events and that determinations of location were better than for the VSN system. For inland earthquakes, both systems had location errors less than 10 km. On the other hand, for offshore earthquakes, the VSN system missed two events and displayed larger location errors of approximately 50–100 km. On average, the epicenter errors of the *e*BEAR and VSN systems are 10.0 and 16.2 km, respectively. When considering depth determinations, the VSN displayed better results than the *e*BEAR system because the VSN system used both *P*- and *S*-wave arrivals, whereas the *e*BEAR system only used *P*-wave arrivals (Fig. 7a,b). For magnitude determinations, the *e*BEAR system yielded a smaller standard deviation (0.2) compared to the VSN system, with a standard deviation of 0.5 (Fig. 8a,b). The solid circles represent the events detected by both systems; the open circles represent the events only detected by the *e*BEAR system. If we only compare the solid circles, it also shows the *e*BEAR system has better magnitude estimations than the VSN system. In the comparison of reporting times, Figure 9a,b indicates that almost every earthquake processed by the *e*BEAR system displayed an earlier reporting time. On average, the *e*BEAR system shortens reporting times by 3.2 and 5.5 s, compared to the VSN system for inland and offshore earthquakes, respectively. Because the *e*BEAR system contains 149 seismic stations distributed in a smaller station coverage gap and because station locations are denser than the VSN system based on 110 stations, the *e*BEAR system can obtain an EEW report more efficiently than the VSN system. Moreover, for an earthquake that occurred in the southern Taiwan offshore area, the station distributions of the *e*BEAR system and the VSN system are similar, but the difference of the reporting time is about 9 s (Fig. 9). This indicates the *e*BEAR system can be operated more efficiently than the VSN system without considering the influence of the station distribution. Figure 10 provides warning times to target areas in metropolitan Taipei. Warning time is defined as the time between the reporting time and the arrival of the *S* wave. The *e*BEAR system provides a longer warning time than the VSN system. For the eastern offshore area of Taiwan, the *e*BEAR system can provide a warning time that is 5 s longer, on average, than the VSN system. The major reason is that by adding the MACHO system and the YOJ station into the seismic network, the *e*BEAR

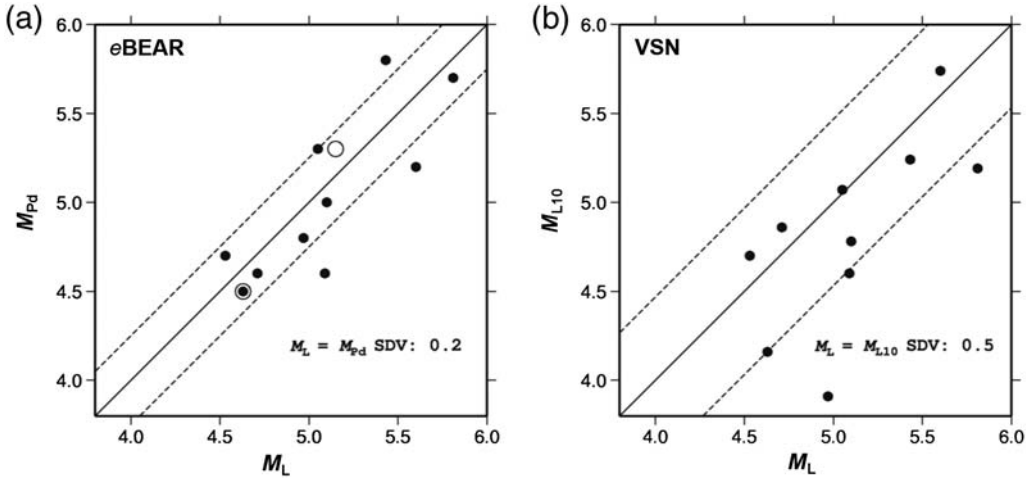

Figure 8. Magnitude estimations as compared to online performance between the *e*BEAR and VSN systems: (a) results from the *e*BEAR system and (b) results from the VSN system. The solid circles represent the events detected by the *e*BEAR and VSN systems. The open circles represent the events only detected by the *e*BEAR system. The solid line represents the 1:1 line. Dashed lines represent one standard deviation.

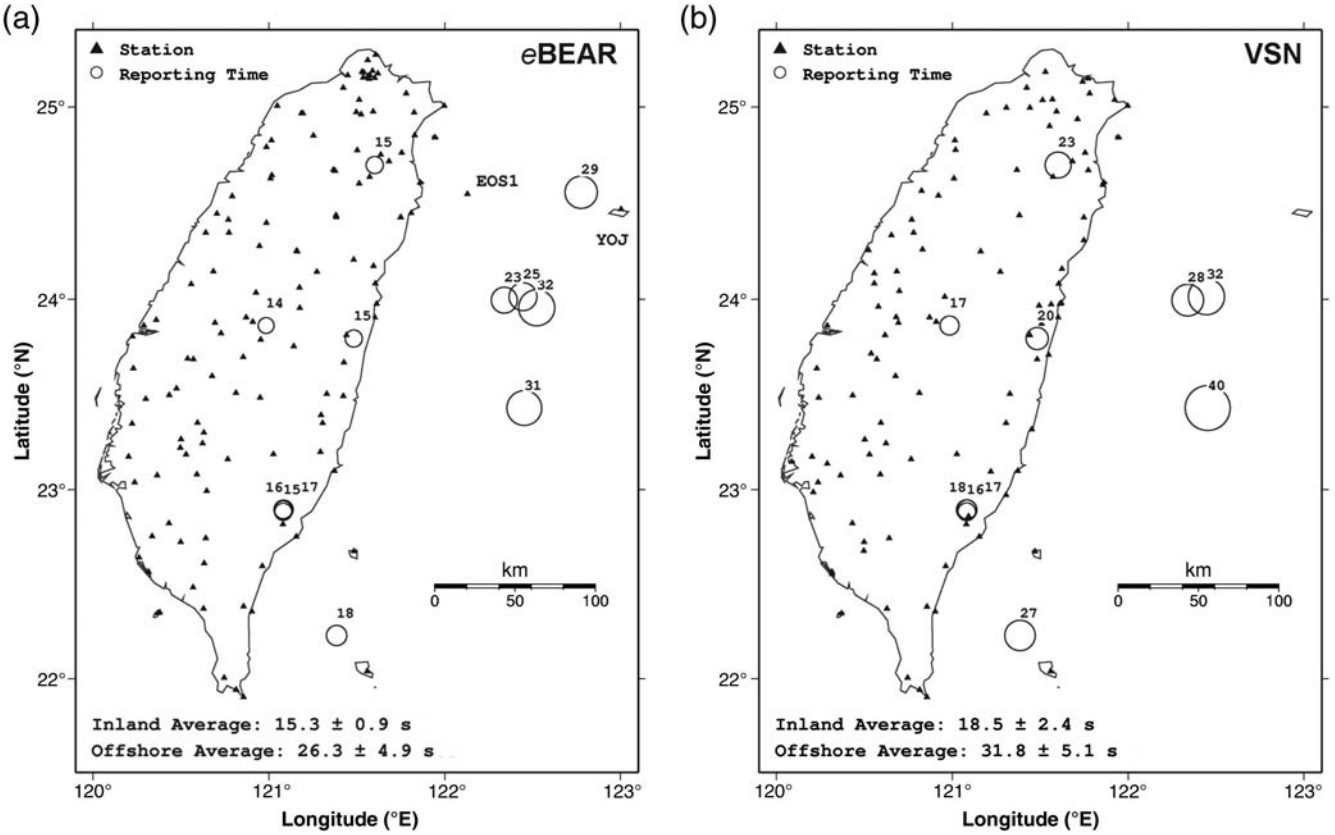

Figure 9. The reporting time comparison for online performance between the *e*BEAR and VSN systems: (a) results from the *e*BEAR system using 149 stations within the CWBSN, and (b) results from the VSN system using 110 real-time data stream (RTD) stations.

system has a smaller station coverage gap. In addition, for events with the approximate locations of the 1999 M_w 7.6 Chi-Chi earthquake and the 2002 M_w 7.1 eastern Taiwan offshore earthquake, the Taipei metropolitan area would have had a warning time of 26 and 15 s, respectively.

EEW Disseminations of the *e*BEAR System

The *e*BEAR system has issued EEW warnings to about 3600 junior and senior high schools in Taiwan since January 2014. Those schools receive warnings from the CWB and

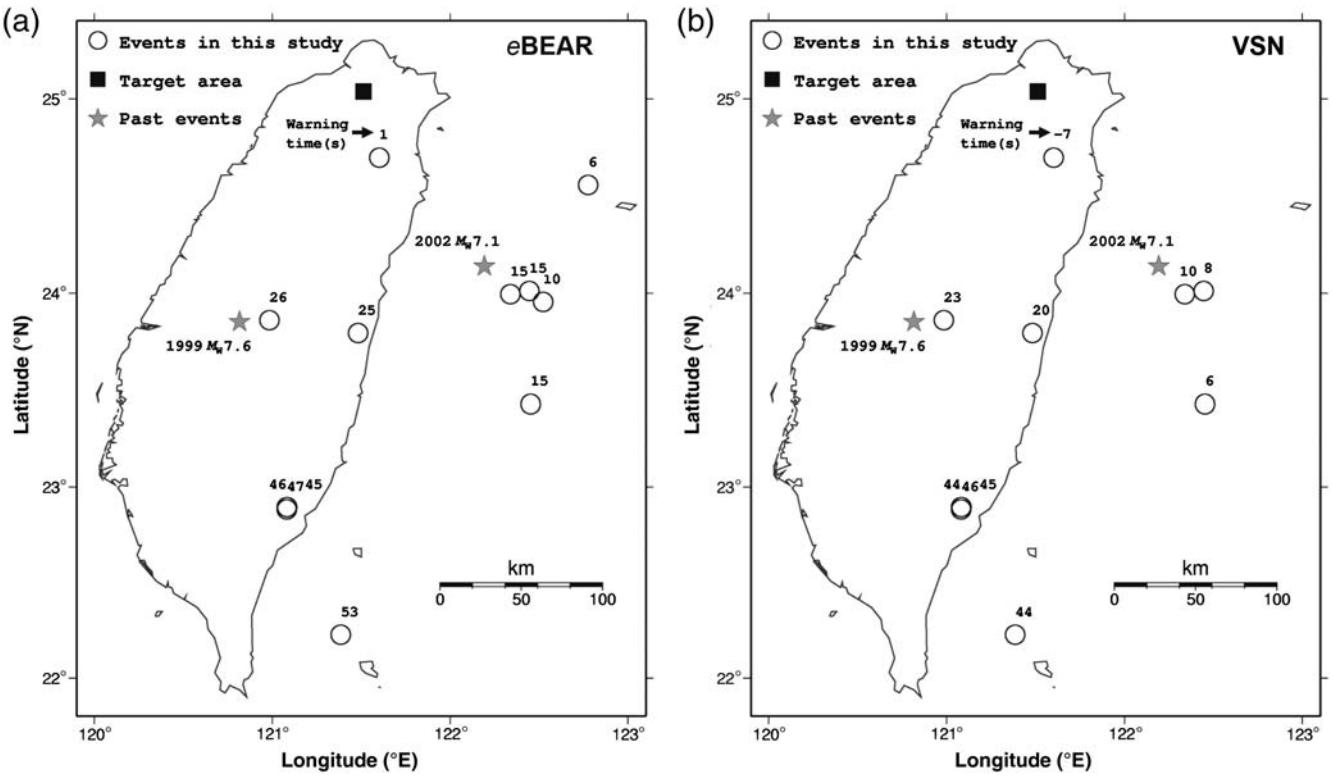

Figure 10. Warning time comparisons for online performance between the *e*BEAR and VSN systems: (a) results from the *e*BEAR system using 149 stations, and (b) results from the VSN system using 110 RTD stations. The solid square represents the target area for obtaining warnings, and open circles represent epicenters. The number over the open circle is the warning time, defined as the time between the reporting time and the arrival of the *S* wave. If the warning time value is negative, the target area has no warning time.

transfer messages to their broadcast system using a user-display software, shown in Figure 4. From January 2014 to September 2014, there are 28 earthquakes with magnitude greater than 4.5 and depth less than 40 km reported by the CWB. The *e*BEAR system has reported 20 events and missed 8 events. Figure 11 shows the epicenters distribution of the reported and missed events, as well as the reporting times of the *e*BEAR system. All of the missed events are located on the offshore area. For the reported events, the average location error is 4.7 ± 2.9 km and the average magnitude error is 0.2 ± 0.1. The 21 May 2014 Hualien earthquake with local magnitude 6.0 is the largest event during this period. The *e*BEAR system issued the alert 15.4 s after the earthquake occurrence. It can provide about 25 s leading time for the Taipei area.

Since January 2014, there have been two false alerts issued by the system. Neither false alert was caused by false triggers. Instead, improper operation caused the false alerts to be generated and sent to the schools. The first false alarm was caused by performing an offline test; because the offline and the online systems run on the same computer, the result of the offline test was sent to the online reporting system and caused a false alert. To avoid this kind of false alarm, we separated the offline and online systems.

The second false alarm was caused by the Earthworm communication modules that provide a rapid message exchange facility between two Earthworm processing systems. When the earthquake occurred, the EEW1 determined the source parameters and sent them to the DCSN using the communication modules, as shown in Figure 3. However, the EEW message could not be sent (and instead was stored in the memory) because the connection between the communication modules was broken. When the system operator found the connection problem and restarted them several hours later, they were reconnected again. As a result, the source parameters were received by the DCSN. The alert was then sent to the schools, but it was delayed for several hours after the earthquake occurred. To solve the connection problem, we started to monitor heartbeat debug messages, which is a hand-shaking procedure between the communication modules. The system operator can figure out the connection problems and fix them before the system is triggered by earthquakes.

Discussion and Conclusions

In general, station coverage gap is a key factor for controlling performance within the *e*BEAR system. If an earthquake is detected by a group of seismic stations with a smaller station coverage gap, the EEW system is capable of high-quality hypocenter estimations and the rms of the travel-time residuals is smaller (Wu, Chang, *et al.*, 2013).

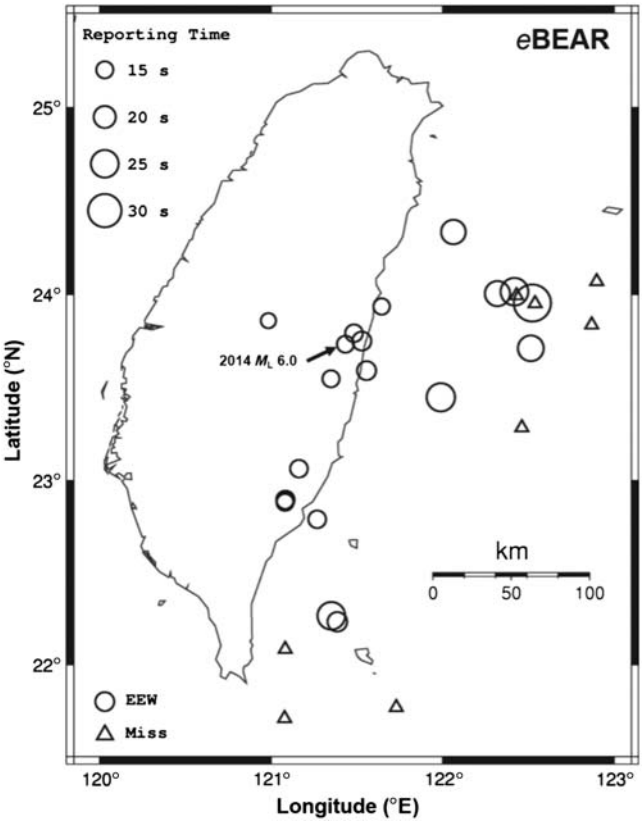

Figure 11. EEW disseminations of the *e*BEAR system. There are 28 events with magnitude greater than 4.5 and depth less than 40 km from January 2014 to September 2014. The *e*BEAR system reported 20 events, indicated as open circles. The size of circles corresponds to the reporting time. Eight events were not reported by the *e*BEAR system (open triangles). During this period the largest event occurred in the Hualien area, with local magnitude 6.0 and reported at 15.4 s after the earthquake occurrence.

For reliable magnitude estimations, good station coverage also reduces directivity effects by averaging the magnitudes of different stations that surround the epicenter. Moreover, because stable results of the EEW system can be obtained earlier, the EEW system is capable of reducing response times. The CWBSN is broader and the distribution denser than the RTD. Therefore, *e*BEAR system performance for location, magnitude, and reporting time are better than for the VSN.

Compared to the CWB catalog, the magnitude of the standard deviation for estimations of moderate-sized earthquake magnitudes in the *e*BEAR system is 0.3, indicating that the magnitude estimations are good for EEW purposes. However, it is difficult to predict earthquake magnitudes of large events within a few seconds of early *P* waves (Hoshiba and Iwakiri, 2011; Colombelli *et al.*, 2012). Once a large earthquake occurs, the rupture process is not approximately a point-source problem. The majority of released energy during the rupture process may not occur at the beginning of the rupture. Therefore, only acquiring information a few seconds after *P*-wave arrival is not enough for estimating the entire energy from an event. Magnitude growth must be tracked and updated over time.

In Taiwan, the VSN system has operated and issued warnings to specific agencies for more than 10 years. The technology for data processing and information transmission is not efficient. The current system consists of a series of computers, programmed for individual tasks that are connected to one another (Wu and Teng, 2002). Using a Windows-based personal computer (Microsoft Corporation), tasks include data acquisition, phase picking, and determinations of earthquake location and magnitude. Each computer archives its result in text files and moves these files to another computer for delivering messages. The procedure takes time to produce files and increases the reporting time after an earthquake occurs. In contrast, Earthworm exchanges messages more efficiently. Earthworm communicates between modules with shared memory regions on local computers and transmission control protocol/IP protocols on remote computers. In this work, the *e*BEAR system was improved based on a comparison of the VSN system. Because of the use of the *P*-wave method and an increase in station density and coverage using the Earthworm configuration, the *e*BEAR system is capable of providing fast and robust EEW information. On average, the reporting time for inland earthquakes occurs within approximately 16 s and for offshore earthquakes occurs within approximately 27 s, indicating that the radius of the blind zone area is approximately 60 km for inland events and 100 km for offshore events. However, some eastern offshore events have an approximate 27 s reporting time and could still provide enough of a warning time for inland regions if a large earthquake occurs. In the future, it is possible to further reduce the reporting time by deploying more seismic stations in the mountainous areas of Taiwan so that the geometry of the seismic network is more evenly distributed.

The *e*BEAR system is a portable package within Earthworm. Any seismic network containing Earthworm is easy to operate with the *e*BEAR system. Therefore, the low cost EEW network of Taiwan, named *P*-alert, running in Earthworm with more than 500 stations (Wu, Chen, *et al.*, 2013; Hsieh *et al.*, 2014; Wu, 2014), is the next candidate to test with the *e*BEAR system. If the CWBSN and *P*-alert seismic networks are merged together, the density and coverage of seismic stations will be greatly enhanced. With an enhanced network, reporting times can be reduced further with the *e*BEAR system. In addition, providing more robust measurements of magnitudes can be estimated easily using initial *P*-wave amplitudes and their spatial distributions (Lin *et al.*, 2011).

Data and Resources

The records used in this study were collected from the Central Weather Bureau Seismic Network of Taiwan. Access to waveform records can be obtained from the owners upon request (http://www.cwb.gov.tw/eng/index.htm; last accessed December 2014).

Acknowledgments

We would like to thank three anonymous reviewers for providing constructive comments. Earthworm (Johnson *et al.*, 1995) and Generic Mapping Tools (GMT; Wessel and Smith, 1998) software programs were used in this study and are gratefully acknowledged. Our work was supported by the Ministry of Science and Technology, Taiwan.

References

Allen, R. M., P. Gasparini, O. Kamigaichi, and M. Böse (2009). The status of earthquake early warning around the world: An introductory overview, *Seismol. Res. Lett.* **80,** 682–693, doi: 10.1785/gssrl.80.5.682.

Chang, C. H., Y.-M. Wu, D.-Y. Chen, T.-C. Shin, T.-L. Chin, and W.-Y. Chang (2012). An examination of telemetry delay in the Central Weather Bureau Seismic Network, *Terr. Atmos. Ocean. Sci.* **23,** 261–268.

Chen, D.-Y., T. L. Lin, Y.-M. Wu, and N.-C. Hsiao (2012). Testing a *P*-wave earthquake early warning system by simulating the 1999 Chi-Chi, Taiwan, M_w 7.6 earthquake, *Seismol. Res. Lett.* **83,** 103–108, doi: 10.1785/gssrl.83.1.103.

Colombelli, S., A. Zollo, G. Festa, and H. Kanamori (2012). Early magnitude and potential damage zone estimates for the great M_w 9 Tohoku-Oki earthquake, *Geophys. Res. Lett.* **39,** L22306, doi: 10.1029/2012GL053923.

Hoshiba, M., and K. Iwakiri (2011). Initial 30 seconds of the 2011 Off the Pacific Coast of Tohoku earthquake (M_w 9.0)—Amplitude and tau(c) for magnitude estimation for earthquake early warning, *Earth Planets Space* **63,** 553–557.

Hsiao, N.-C., T.-W. Lin, S.-K. Hsu, K.-W. Kuo, T.-C. Shin, and P.-L. Leu (2013). Improvement of earthquake locations with the Marine Cable Hosted Observatory (MACHO) offshore NE Taiwan, *Mar. Geophys. Res.* doi: 10.1007/s11001-013-9207-3.

Hsiao, N.-C., Y.-M. Wu, T.-C. Shin, L. Zhao, and T.-L. Teng (2009). Development of earthquake early warning system in Taiwan, *Geophys. Res. Lett.* **36,** L00B02, doi: 10.1029/2008gl036596.

Hsiao, N.-C., Y.-M. Wu, L. Zhao, D.-Y. Chen, W.-T. Huang, K.-H. Kuo, T.-C. Shin, and P.-L. Leu (2011). A new prototype system for earthquake early warning in Taiwan, *Soil Dynam. Earthq. Eng.* **31,** 201–208, doi: 10.1016/j.soildyn.2010.01.008.

Hsieh, C. Y., Y. M. Wu, T. L. Chin, K. H. Kuo, D. Y. Chen, K. S. Wang, Y. T. Chan, W. Y. Chang, W. S. Li, and S. H. Ker (2014). Low cost seismic network practical applications for producing quick shaking maps in Taiwan, *Terr. Atmos. Ocean. Sci.* **25,** 617–624, doi: 10.3319/TAO.2014.03.27.01(T).

Huang, H. H., Y. M. Wu, T. L. Lin, W. A. Chao, J. B. H. Shyu, C. H. Chan, and C. H. Chang (2011). The preliminary study of the 4 March 2010 M_w 6.3 Jiasian, Taiwan, earthquake sequence, *Terr. Atmos. Ocean. Sci.* **22,** 283–290, doi: 10.3319/TAO.2010.12.13.01(T).

Huang, Y. L., B. S. Huang, K. L. Wen, Y. C. Lai, and Y. R. Chen (2010). Investigation for strong ground shaking across the Taipei basin during the M_w 7.0 eastern Taiwan offshore earthquake of 31 March 2002, *Terr. Atmos. Ocean. Sci.* **21,** 485–493, doi: 10.3319/TAO.2009.12.11.01(TH).

Johnson, C. E., A. Bittenbinder, B. Bogaert, L. Dietz, and W. Kohler (1995). Earthworm: A flexible approach to seismic network processing, *IRIS Newsletter* **14,** 4.

Lin, T. L., Y. M. Wu, and D. Y. Chen (2011). Magnitude estimation using initial *P*-wave amplitude and its spatial distribution in earthquake early warning in Taiwan, *Geophys. Res. Lett.* **38,** L09303, doi: 10.1029/2011GL047461.

Shin, T.-C., and T.-l. Teng (2001). An overview of the 1999 Chi-Chi, Taiwan, earthquake, *Bull. Seismol. Soc. Am.* **91,** 895–913, doi: 10.1785/0120000738.

Shin, T.-C., C.-H. Chang, H.-C. Pu, H.-W. Lin, and P.-L. Leu (2013). The geophysical database management system in Taiwan, *Terr. Atmos. Ocean. Sci.* **24,** 11–18.

Teng, T. L., L. Wu, T. C. Shin, Y. B. Tsai, and W. H. K. Lee (1997). One minute after: Strong-motion map, effective epicenter, and effective magnitude, *Bull. Seismol. Soc. Am.* **87,** 1209–1219.

Wessel, P., and W. H. F. Smith (1998). New, improved version of Generic Mapping Tools released, *EOS Trans. AGU.* **79,** 579.

Wu, Y. M. (2014). Progress on development of an earthquake early warning system using low cost sensors, *Pure Appl. Geophys.* doi: 10.1007/s00024-014-0933-5.

Wu, Y.-M., and T.-L. Teng (2002). A virtual subnetwork approach to earthquake early warning, *Bull. Seismol. Soc. Am.* **92,** 2008–2018.

Wu, Y.-M., and L. Zhao (2006). Magnitude estimation using the first three seconds *P*-wave amplitude in earthquake early warning, *Geophys. Res. Lett.* **33,** doi: 10.1029/2006gl026871.

Wu, Y. M., C. H. Chang, H. Kuo-Chen, H. H. Hunag, and C. Y. Wang (2013). On the use of explosion records for examining earthquake location uncertainty in Taiwan, *Terr. Atmos. Ocean. Sci.* **24,** 685–694, doi: 10.3319/TAO.2013.01.31.01(T).

Wu, Y. M., D. Y. Chen, T. L. Lin, C. Y. Hsieh, T. L. Chin, W. Y. Chang, W. S. Li, and S. H. Ker (2013). A high-density seismic network for earthquake early warning in Taiwan based on low-cost sensors, *Seismol. Res. Lett.* **84,** 1048–1054, doi: 10.1785/0220130085.

Wu, Y.-M., J.-K. Chung, T.-C. Shin, N.-C. Hsiao, Y.-B. Tsai, W. H. K. Lee, and T.-l. Teng (1999). Development of an integrated earthquake early warning system in Taiwan—Case for Hualien area earthquakes, *Terr. Atmos. Ocean. Sci.* **10,** 719–736.

Wu, Y. M., W. H. K. Lee, C. C. Chen, T. C. Shin, T. L. Teng, and Y. B. Tsai (2000). Performance of the Taiwan Rapid Earthquake Information Release System (RTD) during the 1999 Chi-Chi (Taiwan) earthquake, *Seismol. Res. Lett.* **71,** 338–343.

Wu, Y.-M., T.-L. Lin, W.-A. Chao, H.-H. Huang, N.-C. Hsiao, and C.-H. Chang (2011). Faster short-distance earthquake early warning using continued monitoring of filtered vertical displacement: A case study for the 2010 Jiasian, Taiwan, earthquake, *Bull. Seismol. Soc. Am.* **101,** 701–709, doi: 10.1785/0120100153.

Wu, Y.-M., T.-C. Shin, C.-C. Chen, W. H. K. Lee, and T. L. Teng (1997). Taiwan rapid earthquake information release system, *Seismol. Res. Lett.* **68,** 931–943.

Wu, Y. M., T. C. Shin, and Y. B. Tsai (1998). Quick and reliable determination of magnitude for seismic early warning, *Bull. Seismol. Soc. Am.* **88,** 1254–1259.

Yu, S. B., H. Y. Chen, L. C. Kuo, S. E. Lallemand, and H. H. Tsien (1997). Velocity field of GPS stations in the Taiwan area, *Tectonophysics* **274,** 41–59.

Central Weather Bureau
No. 64, Kung-Yuan Road
Taipei 10048, Taiwan
(D.-Y.C., N.-C.H.)

Department of Geosciences
National Taiwan University
No. 1, Section 4, Roosevelt Road
Taipei 10617, Taiwan
drymwu@ntu.edu.tw
yihmin.wu@gmail.com
(Y.-M.W.)

Manuscript received 28 May 2014;
Published Online 3 February 2015